

# Research on clock synchronization method of marine controlled source electromagnetic transmitter base on coaxial cable

Zhibin Ren<sup>1</sup>, Meng Wang<sup>1</sup>, Kai Chen<sup>1</sup>, Chentao Wang<sup>1</sup>, Runfeng Yu<sup>1</sup>

<sup>1</sup>China University of Geosciences (Beijing), School of Geophysics and Information Technology, Beijing  
CO 100083, China

*Correspondence to:* Meng Wang (wangmeng@cugb.edu.cn).

**Abstract.** Marine controlled source electromagnetic (MCSEM) method is widely employed to reveal the electrical structure of shallow media below seafloor. It is an indispensable geophysical means in the exploration of marine oil, gas, natural gas hydrates and seafloor geological structures. The transmitter and receiver in electromagnetic detection equipment need to maintain a high temporal consistency, typically relying on high-stability pulse-per-second (PPS) generated by GPS or BeiDou navigation modules. Coaxial cable is a widely used tow cable, so it is necessary to design a clock synchronization method of marine controlled source electromagnetic transmitter using coaxial cable. This paper proposes a method for synchronizing the internal clock of transmitter with PPS using ship-borne power supply when coaxial cable is used as tow cable. In this method, the ship-borne high-power supply outputs a high-voltage alternating current (AC) signal that is synchronized with 400 Hz signal output from GPS; the coaxial cable transmits AC high-power electrical energy and control commands; the AC signal transmitted via coaxial cable is converted into a stable and continuous 1 Hz signal by step-down, waveform shaping and frequency division for synchronizing the internal time pulses of transmitter. The test result shows that 1 Hz signal obtained by this method has a deviation of approximately 504 ns relative to PPS. This deviation meets MCSEM transmitter's requirement for clock synchronization.

**Keywords:** marine controlled source electromagnetic, coaxial cable, transmitter, clock synchronization

## 1 Introduction

Marine controlled source electromagnetic (MCSEM) method is one of the methods in exploration of seafloor natural gas hydrates (Edwards and Chave, 1986; Cox et al., 1986). It is an indispensable geophysical means in the exploration of marine oil, gas, natural gas hydrates and seafloor geological structures (Constable and Srnka, 2007; Constable, 2010). In MCSEM method, the synchronization of internal clocks between transmitter and receiver is an very important issue (Wang et al., 2015b; Meng et al., 2009). Electromagnetic data processing and interpretation depend on synchronization between transmitter and receiver (Qiu et al., 2020). MCSEM transmitter and receiver are separated from each other (Chen et al., 2012; Chen et al., 2020), and they are not connected by any cable. Therefore, Pulse-Per-Second (PPS) signal output from GPS is used as a common synchronization signal to synchronize the internal clock of transmitter and receiver.

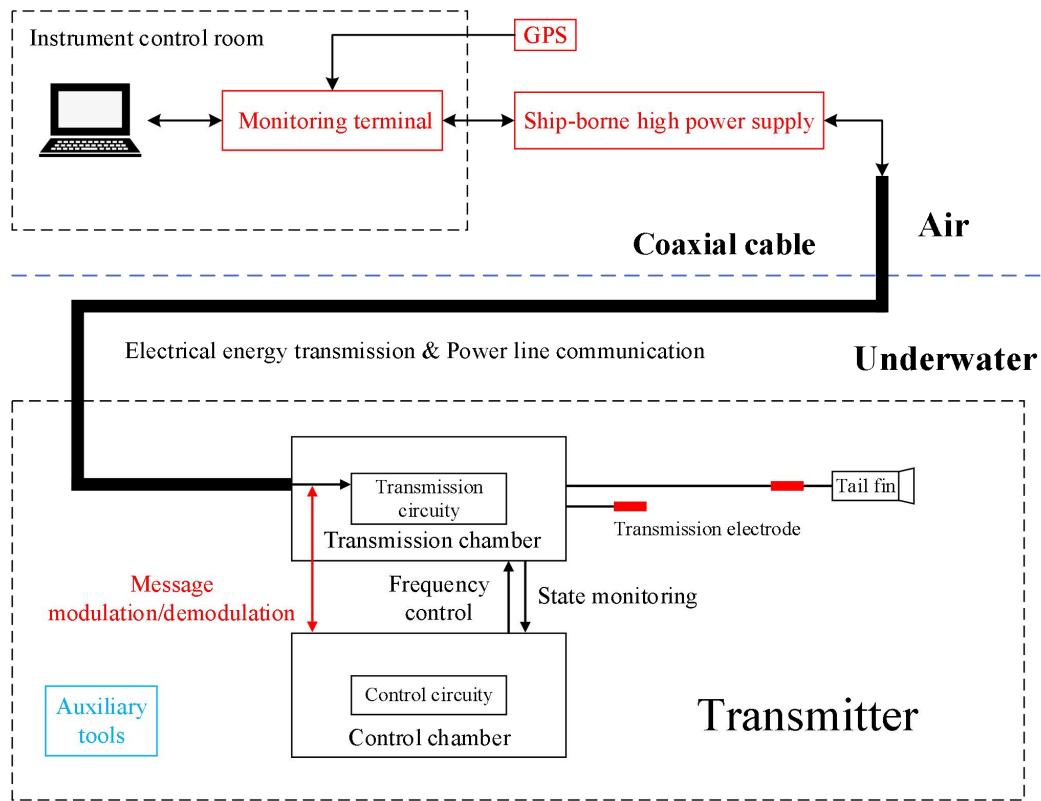
The tow cables commonly used in MCSEM transmission systems are photoelectric composite cables and coaxial cables. The transmitter's clock synchronization method varies based on the type of tow cable. When using coaxial cable as tow cable, clock synchronization can be achieved by controlling power supply output or transmitting PPS to transmitter before it is submerged. As an example, SUESI-500 transmitter of Scripps Institution of Oceanography uses a standard UNOLS 0.680 inch

42 (17.27 mm) coaxial cable as tow cable. They use a 400 Hz output from a GPS clock to generate a 400  
43 Hz sine wave of variable amplitude to control power supply (Constable, 2013; Constable, 2006). The  
44 clock information in power signal serves as a reference for clock-related operations within transmitter.  
45 SUESI-500 transmitter's frequency control signals is generated based on 400 Hz signal. When using  
46 photoelectric composite cable as tow cable, clock synchronization can be achieved by transmitting PPS  
47 through one channel of optical fiber. For example, the transmitter of China University of Geosciences  
48 (Beijing) uses a 32.8 mm photoelectric composite cable as tow cable, and its clock synchronization is  
49 achieved by transmitting PPS and GPS time through optical fiber (Wang et al., 2021). However, the  
50 cost of photoelectric composite cable is high and generally only large scientific research ships can be  
51 equipped. In order to enable MCSEM transmitters work on a wider variety of ships, using coaxial cable  
52 is necessary. Compared to photoelectric composite cable, coaxial cable has only one message channel  
53 and can't be assigned a separate channel to transmit PPS. The coaxial cable can transmit data and  
54 commands using power line communication, but its delay is unstable. If PPS is transmitted via coaxial  
55 cable, it will have a large deviation. Consequently, how to use coaxial cable to synchronize internal  
56 clock of MCSEM transmitter is a challenging problem. This paper proposes a clock synchronization  
57 method of MCSEM transmitter based on coaxial cable. In this method, the sinusoidal signal from  
58 power supply is synchronized with 400 Hz square wave signal from GPS. Then the sinusoidal power  
59 signal transmitted to underwater transmitter is converted into a stable and continuous 1 Hz square wave  
60 signal by step-down, waveform shaping and frequency division. The final 1 Hz square wave signal is as  
61 the synchronization signal for transmitter's internal clock.

## 62 **2 Clock synchronization based on coaxial cable**

63 In this paper, the tow cable used is coaxial cable. This coaxial cable not only transmits electrical energy  
64 but also functions as a communication link between deck monitoring terminal and underwater  
65 transmitter. Communication is achieved through power line communication technology (Ferreira et al.,  
66 2001; Amuta et al., 2020; Kaddoum and Tadayon, 2016). The power transmitted through coaxial cable  
67 is a 400 Hz sinusoidal waveform.

68 Fig.1 illustrates the schematic diagram of MCSEM transmission system, which is based on coaxial  
69 cable. The ship is equipped with an instrument control room used to house personal computer (PC) and  
70 deck monitoring terminal. The deck monitoring terminal is connected to the ship-borne high-power  
71 supply, allowing it to control power on/off functions and communication with underwater transmitter.  
72 It also receives GPS time messages and PPS for clock synchronization. The ship-borne high-power  
73 supply generates 0~3000 V, 400 Hz alternating current (AC) electricity to power underwater  
74 transmitter (Wang et al., 2017b). In addition to transmitting electrical energy, the coaxial cable also  
75 transmits commands to underwater transmitter by power line communication. The underwater  
76 transmitter consists of two main components: a transmission chamber and a control chamber. The  
77 transmission chamber contains step-down, rectification and inverter units, which transmit high power  
78 electromagnetic waves to the seafloor (Wang et al., 2015a). The control chamber contains control  
79 circuit of entire transmitter, allowing it to transmit frequency-switching signals to control high-current  
80 transmission and monitor transmitter's state parameters. The transmitter is also equipped with auxiliary  
81 tools such as an altimeter and an attitude module to measure safety-related parameters during  
82 underwater towing. Behind the transmitter, two electrodes are towed, with a tail fin attached to the  
83 electrodes to stabilize their orientation (Wang et al., 2013; Wang et al., 2017a; Liu et al., 2012).

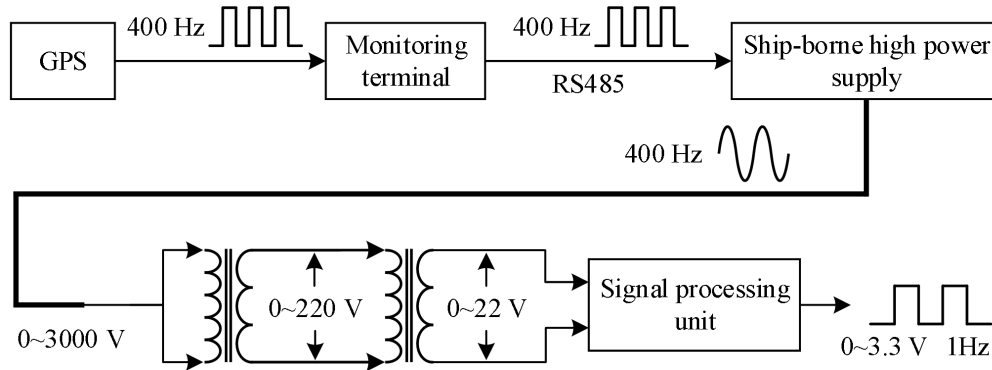


84

85 **Fig.1 The schematic diagram of MCSEM transmission system based on coaxial cable.**

86

87 Fig.2 illustrates the synchronization signal flow based on coaxial cable. The GPS module features a  
 88 TIMEPULSE pin that can be configured to output a 400 Hz square wave, with its rising edges precisely  
 89 aligned with PPS at integer seconds. The 400 Hz square wave is transmitted to the ship-borne  
 90 high-power supply through deck terminal as a synchronization signal. To prevent interference from  
 91 high-power supply, the signal between deck monitoring terminal and power supply is transmitted via  
 92 an isolated RS485 bus. The 400 Hz sinusoidal signal generated by high-power supply is transmitted to  
 93 underwater transmitter through coaxial cable, where it is converted to a sinusoidal signal in the range of  
 94 0~22 V by two transformers. The signal processing unit in transmitter's control circuit processes the  
 95 0~22 V sinusoidal signal and generates a 1 Hz square wave as the synchronization signal for control  
 96 circuit. The rising edges of 1 Hz square wave are aligned with the rising edges of PPS.



97

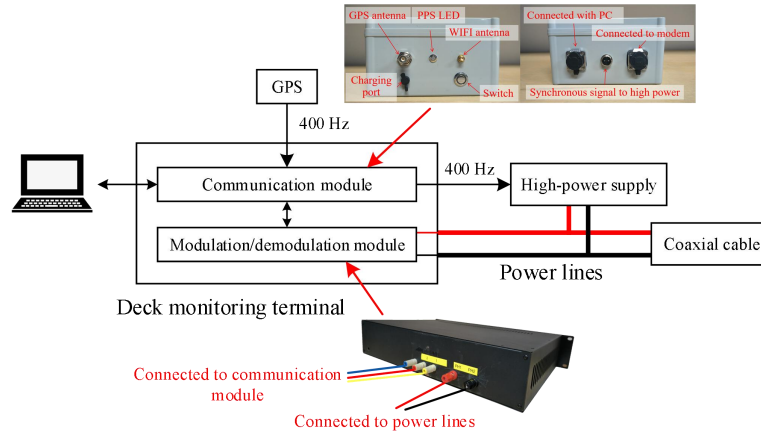
98 **Fig.2 The flow diagram of synchronization signal.**

99

100 **3 Hardware design of clock synchronization method based on coaxial cable**

101 **3.1 Deck monitoring terminal**

102 Fig.3 shows the block diagram of deck monitoring terminal. The deck monitoring terminal comprises a  
103 communication module and a coaxial cable modulation/demodulation module (modem). The  
104 communication module is responsible for interaction between monitoring software on PC and  
105 transmitter. A signal follower within communication module receives 400 Hz signal from GPS and  
106 relays it to high power supply as a synchronization signal. The coaxial cable modem modulates  
107 messages sent by PC onto two power lines of coaxial cable and demodulates messages returned by  
108 transmitter through coaxial cable.



109

110

**Fig.3 The block diagram of deck monitoring terminal.**

111

112 **3.2 High-power supply output synchronized with GPS**

113 The high-power supply is designed with a function to accept external synchronization signals. Both the  
114 underwater transformers of transmitter and ship-borne high-power supply operate at a frequency of 400  
115 Hz. Accordingly, the TIMEPULSE pin of GPS is configured to output a 400 Hz signal and is  
116 connected to high-power supply via a RS485 module. This RS485 module will introduce a certain  
117 delay. Fig.4 shows the comparison of PPS before and after RS485 transmission. It is observed that the  
118 delay introduced by RS485 is less than 50 ns. The power supply output voltage is set to 20 V. The  
119 TIMEPULSE pin on another GPS is configured to output a 1 Hz signal, which is monitored alongside  
120 the power supply output. Fig.5 shows the synchronized output signal waveform of power supply. It can  
121 be observed that the zero phase of power supply output signal is aligned with the rising edge of PPS.  
122 After continuous observation, the 400 Hz sinusoidal signal output from power supply remains stable  
123 relative to the rising edges position of PPS. This synchronization of power supply output is effective,  
124 and forms the foundation of entire clock synchronization method.

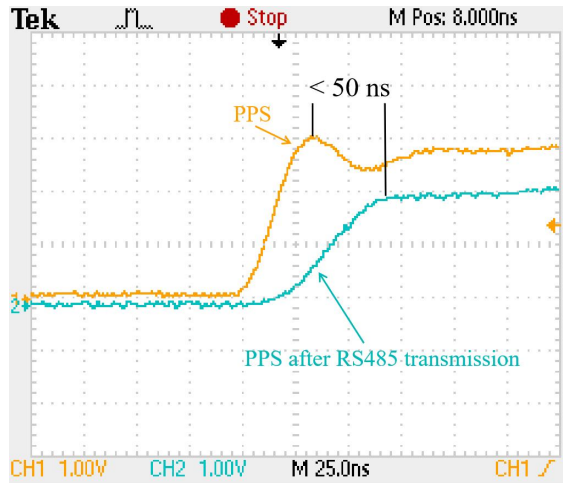


Fig.4 The comparison of PPS before and after RS485 transmission.

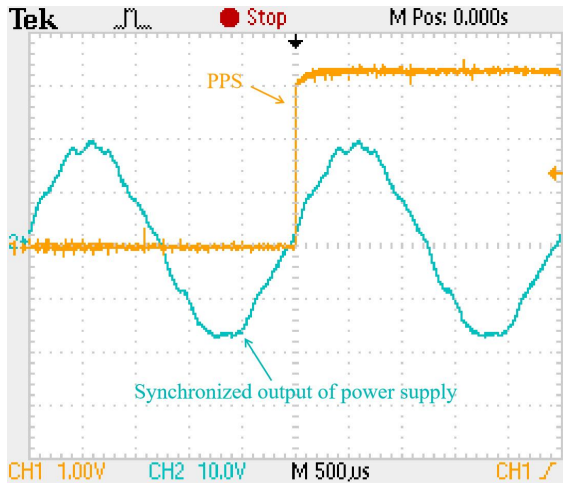


Fig.5 The synchronized output signal waveform of power supply.

### 3.3 Signal processing unit

The 400 Hz sinusoidal signal output from high-power supply is transmitted to transmitter via a coaxial cable. Then it passes through two transformers and is converted into a sinusoidal wave with an amplitude ranging from 0 to 24 V. This signal is converted into 1 Hz square wave with an amplitude of 0 to 3.3 V by signal processing circuit. Fig.6 shows the hardware of signal processing unit.

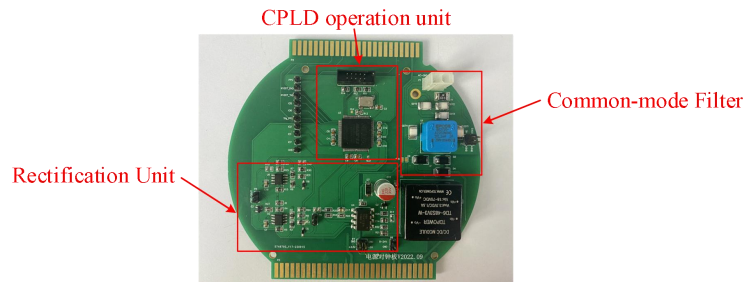
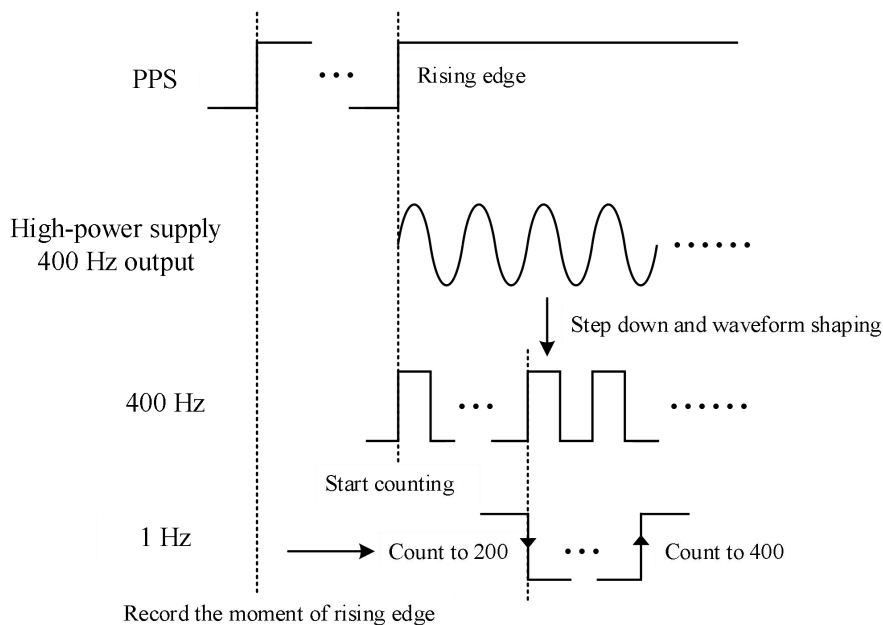


Fig.6 The hardware of signal processing unit.

138

139 The 400 Hz sinusoidal wave, ranging from 0 to 24 V, is first processed by a common-mode filter to  
140 eliminate noise. A protective circuit consisting of gas discharge tubes (GDT) and transient voltage  
141 suppression (TVS) diodes, surrounds common-mode filter circuit to prevent over-voltage and protect  
142 subsequent stages. After filtering, the sinusoidal wave is processed through a rectification unit, which  
143 converts it into a 0~3.3 V, 400 Hz square wave signal. This rectification unit comprises an optical  
144 coupler and an operational amplifier, which rectifies signal, isolates input from output, and protects  
145 following operational circuits from sudden variations in the input signal. The square wave signal from  
146 rectifier is then processed by the operation unit of underwater signal processing system, which  
147 generates a 1 Hz square wave using a pulse counting method. The core of operation unit is a complex  
148 programmable logic device (CPLD), which outputs one rising edge for every 400 counted rising edges  
149 of 400 Hz square wave. The 1 Hz square wave output by CPLD operation unit is the final  
150 synchronization signal transmitted to control circuit.

151 To align the rising edges of 1 Hz square wave with the rising edges of PPS, CPLD module records the  
152 exact moment of PPS rising edges. The 1 Hz square wave is aligned with PPS only when CPLD begins  
153 counting 400 Hz square wave at the moment of a certain PPS rising edge. Therefore, before  
154 submerging transmitter, an external GPS module is connected to it. Once CPLD records the timing of  
155 PPS rising edges, it generates an internal 1 Hz signal synchronized with PPS. Afterward, the external  
156 GPS module is removed, and power supply is activated. CPLD module initially sets output pin to low  
157 and then raises it high upon detecting the first rising edge of internally generated 1 Hz signal, as  
158 illustrated in Fig.7. After this, when the rising edge count of 400 Hz signal reaches 200, output pin  
159 is set to low, generating a falling edge; when the count of 400 Hz signal reaches 400, output pin is set to  
160 high, generating a rising edge and resetting counter for next cycle. The clock synchronization of entire  
161 transmitter system depends on the rising edges of PPS, which must be generated with accuracy and  
162 stability. Therefore, this method of counting rising edges of 400 Hz signal directly to 400 ensures  
163 precise generation of these rising edges.



164

165

166

**Fig.7 The schematic diagram of 1Hz synchronized signal generation.**

#### 167 4 Analysis of clock synchronization deviation

168 No matter which clock synchronization method is used, there will be a deviation between the final 1 Hz  
169 square wave signal generated and the PPS from GPS. The main deviation in conventional MCSEM  
170 clock synchronization method comes from the crystal oscillator inside transmitter. The generation of 1  
171 Hz signal synchronized with the rising edges of PPS relies on internal crystal oscillator. If the  
172 temperature drift of crystal is smaller, the frequency of output signal is more stable and the clock  
173 synchronization deviation is also smaller. The clock synchronization method in this paper generates a 1  
174 Hz signal synchronized to the rising edges of PPS by counting the rising edges of 400 Hz square wave.  
175 Its frequency stability primarily is from the stability of 400 Hz output of power supply, reducing  
176 dependence on the internal crystal oscillator. The deviation of this method comes from circuit  
177 processing, cable transmission and other stages that may generate signal delay, and it can be calculated  
178 by the following formula:

$$179 \quad T = T_1 + T_2 + T_3 \quad (1)$$

180 where  $T$  is the delay of generated 1 Hz square wave signal relative to PPS,  $T_1$  is the delay generated  
181 by circuit processing stage,  $T_2$  is the delay generated by cable transmission,  $T_3$  is the delay caused  
182 by signal passing through transformers.  $T_1$  mainly consists of three parts: chip program processing,  
183 signal transmission in all circuit, the synchronization process of power supply.  $T_1$  can be calculated  
184 by the following formula:

$$185 \quad T_1 = T_c \times n + t_1 + t_2 \quad (2)$$

186 where  $T_c$  is the instruction cycle of chip, i.e., the time required to execute one instruction, and  $n$  is  
187 the number of instructions,  $t_1$  is the delay caused by signal transmission in all circuit,  $t_2$  is the delay  
188 generated by high-power supply synchronization output.  $T_c$  is related to the crystal oscillator used by  
189 chip. In this paper, the value of  $T_c$  is 6 ns, the value of  $n$  doesn't exceed 30.  $t_1$  is related to the  
190 components used in signal transmission path in the circuit board. In this paper, the value of  $t_1$  doesn't  
191 exceed 4 ns. There is a slight delay in the zero phase of 400 Hz signal from power supply relative to the  
192 rising edges of 400 Hz synchronization signal, but the power supply output signal waveform is not a  
193 standard sine wave, making it difficult to precisely identify the zero phase. Therefore, it is difficult to  
194 obtain an accurate result for  $t_2$  through separate test, but subsequent overall deviation test includes  $t_2$ .  
195  $T_2$  mainly consists of three parts: the delay caused by coaxial cable transmission, and delay caused by  
196 wires transmission between circuit boards, and it can be calculated by the following formula:

$$197 \quad T_2 = \frac{L_{cable}}{v_{cable}} + \frac{L_{wire}}{v_{wire}} \quad (3)$$

$$198 \quad v_{cable} = \eta_1 \times c \quad (4)$$

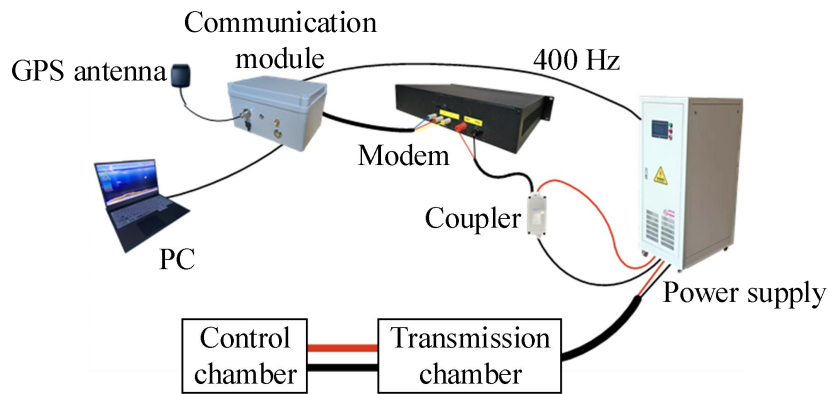
$$199 \quad v_{wire} = \eta_2 \times c \quad (5)$$

200 where  $L_{cable}$  is the length of coaxial cable, and  $v_{cable}$  is the speed at which the signal is transmitted  
201 via coaxial cable,  $L_{wire}$  is the length of wires between circuit boards, and  $v_{wire}$  is the speed at which  
202 the signal is transmitted via wires,  $c$  is the speed of light in a vacuum,  $\eta_1$  is the ratio of signal  
203 transmission speed on coaxial cable to the speed of light in a vacuum,  $\eta_2$  is the ratio of signal  
204 transmission speed between circuit boards via wires to the speed of light in a vacuum. The typical value  
205 of  $\eta_1$  ranges from 0.67 to 0.75, and the typical value of  $\eta_2$  ranges from 0.6 to 0.9 (when using  
206 22AWG wire). Therefore, for every 1 km of coaxial cable, the delay typically falls within a range of  
207 4.48 to 4.98  $\mu$ s. The total length of wires between circuit boards inside transmission chamber doesn't  
208 exceed 1 m, resulting in a delay typically range from 3.7 to 5.56 ns.

209 The 400 Hz signal output from high-power supply passes through two stages of transformers and is  
 210 reduced to low voltage ranging from 0 to 22V for processing by underwater signal processing unit. The  
 211 transformers are not ideal transformers, so there is a certain phase shift between the primary input  
 212 voltage and the secondary output voltage of each transformer, which is the cause of  $T_3$ . Due to limited  
 213 test condition,  $T_3$  can't be tested separately in this paper, but subsequent overall deviation testing  
 214 includes  $T_3$ . All deviations described above can be combined and measured in the overall test of the  
 215 clock synchronization method.

216 **5 The test of clock synchronization method**

217 In accordance with the clock synchronization method using power supply signal based on coaxial cable,  
 218 as discussed in this paper, a test platform was built in laboratory to evaluate the effectiveness of clock  
 219 synchronization. The test setup is shown in Fig.8. Due to the high voltage output of power supply and  
 220 the low voltage requirement of modem, a coupler is needed to connect the two (Giraneza and  
 221 Abo-Al-Ez, 2022; Costa et al., 2017). This coupler is a capacitive coupler, which presents significant  
 222 impedance to 400 Hz AC signal. Consequently, the voltage in power carrier loop primarily accumulates  
 223 at the coupler's ends. Since the frequency of power line communication exceeds 100 kHz, coupler's  
 224 impedance is relatively low. Therefore, the power line communication signal can pass through coupler,  
 225 but the 400 Hz synchronization signal of high-power supply does not. This coupler does not cause a  
 226 delay.



227  
 228 **Fig.8 The diagram of test setup.**  
 229

230 Fig.9 shows the clock synchronization process based on coaxial cable. First, control chamber is  
 231 connected to a GPS module. Once control circuit receives PPS and records the specific timing of rising  
 232 edges, GPS module is removed. Next, high power supply is activated. The 400 Hz AC signal output  
 233 from power supply is converted into 1Hz square wave by the signal processing unit inside control  
 234 chamber. Finally, PC sends a synchronization command and transmitter's internal clock realigns with 1  
 235 Hz square wave.



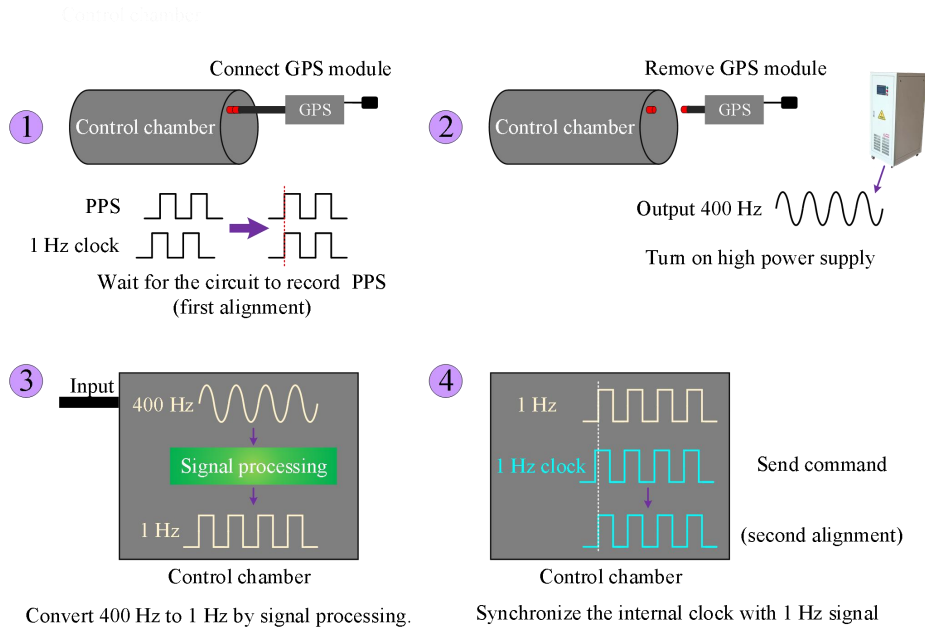


**Fig.9 The clock synchronization process based on coaxial cable.**

236  
 237  
 238  
 239  
 240  
 241  
 242  
 243  
 244  
 245  
 246  
 247  
 248  
 249  
 250  
 251  
 252  
 253  
 254

Fig.10 shows the internal clock synchronized with PPS and the clock synchronization deviation. To facilitate observation, the duty cycle of internal clock signal generated by underwater signal processing unit was set to 50%, while the duty cycle of PPS output from GPS module was set to 40%. After continuous observation, the deviation between the rising edge of internal clock signal and the rising edge of PPS was approximately 504 ns. Fig.11 presents the results of multiple tests, showing that the synchronization deviation fluctuated around 504 ns with a range of 34 ns. The coaxial cable used in test was relatively short. In marine operations, a 10 km length of coaxial cable can introduce a maximum delay of approximately 49.8  $\mu$ s. In this case, the maximum delay of internal clock signal relative to PPS would be approximately 50.3  $\mu$ s. During the measurement of internal clock signal, some interference pulses were observed, likely caused by test pins being too close to high power equipment in laboratory environment. Fig.12 shows some photos of the test scene.

Unlike Scripps transmitter, this study employs a ship-borne high-power supply to transmit 400 Hz signal and generate a 1 Hz square wave synchronized with PPS as the synchronization signal for transmitter circuit. The transmission waveform frequency control signal is generated based on the internal crystal oscillator of circuit, with its rising edge aligned with the rising edge of 1 Hz synchronization signal.

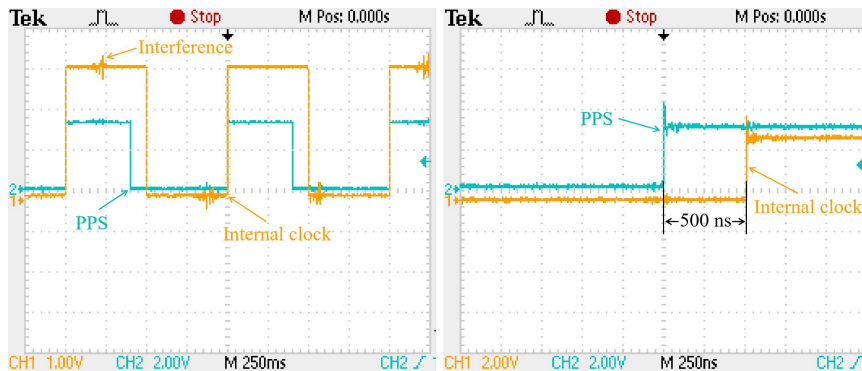
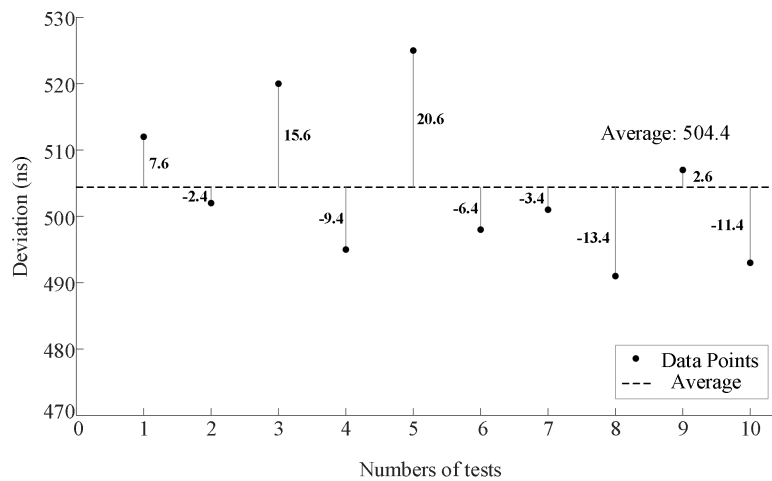


**Fig.10 Internal clock synchronized with PPS (left); clock synchronization deviation (right).**

255  
 256

257



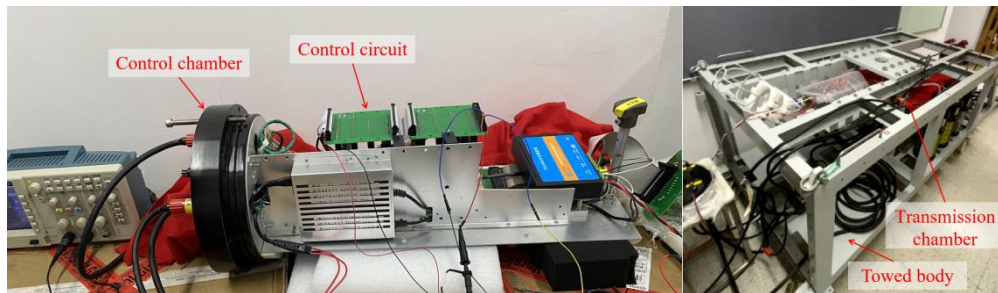
258

259

**Fig.11 The graph of multiple tests results for synchronization deviation, shows the difference between each result and the average value.**

260

261



262

263

**Fig.12 Control chamber (left); transmission chamber (right).**

264

## 265 **6 Conclusion**

266 This paper introduces a clock synchronization method of marine controlled source electromagnetic  
267 transmitter base on coaxial cable and builds related hardware system. In this method, the ship-borne  
268 high power-supply outputs 400 Hz signal synchronized with PPS, and transmits it to underwater  
269 transmitter. The transmitter control circuit can generates a 1 Hz square wave signal synchronized with  
270 PPS for clock synchronization. The delay deviation of 1 Hz square wave signal obtained by this  
271 method relative to PPS is less than 1 ms, which meets the requirement of synchronization accuracy  
272 better than 1 ms in practical operations and can be used for internal clock synchronization of  
273 transmitter. This method can facilitate the use of coaxial cables in MCSEM operations, and expand  
274 transmitter's application scenarios. This method can also provide a reference for the design of other  
275 underwater equipment that uses coaxial cables.

## 276 **7 Statement**

277 This manuscript satisfies the following statements that: 1) all authors agree with the submission, 2) the  
278 work has not been published elsewhere, either completely, in part, or in another form, and 3) the  
279 manuscript has not been submitted to another journal.

## 280 **Data availability**

281 No data sets were used in this article.

## 282 **Author contributions**

283 M. Wang is the project applicant and a key participant in the testing process. K. Chen provided some

284 optimization suggestions for the test scheme. C.T. Wang and R.Y. Yu, as the research assistants, had  
285 helped complete the testing. Z.B. Ren is the project leader, primarily responsible for the test scheme  
286 design, hardware circuit design, and other related tasks.

### 287 **Competing interests**

288 The contact author has declared that none of the authors has any competing interests.

### 289 **Financial support**

290 This work was supported by the National Natural Science Foundation of China (42374221), the Key  
291 Technologies R&D Program (2022YFC2807900), Marine Economic Development in Guangdong  
292 Province (Grant Number: GDNRC[2023]40).

### 293 **Acknowledgement**

294 Thanks to the editors and reviewers. Additionally, this paper was supported by south China sea institute  
295 of oceanology, cas and Fujian earthquake agency. The authors express thanks to the two mentioned  
296 institutions.

### 297 **References**

298 Amuta, E., Awelewa, A., Olajube, A., Somefun, T., Afolabi, G., and Uyi, A.: Power line carrier  
299 technologies: a review, IOP Conference Series: Materials Science and Engineering, Ota, Nigeria,  
300 27th-28th July 2020, 012062, doi: 10.1088/1757-899X/1036/1/012062, 2021.

301 Chen, K., Deng, M., Wu, Z., Jing, J., Luo, X., and Wang, M.: Low Time Drift Technology for Marine  
302 CSEM Recorder, *Geoscience*, 26, 1312-1316, doi: 10.3969/j.issn.1000-8527.2012.06.027, 2012.

303 Chen, K., Deng, M., Yu, P., Yang, Q., Luo, X. H., and Yi, X. P.: A near-seafloor-towed CSEM receiver  
304 for deeper target prospecting, *Terrestrial Atmospheric and Oceanic Sciences*, 31, 565-577, doi:  
305 10.3319/tao.2020.08.03.01, 2020.

306 Constable, S.: Marine electromagnetic methods—A new tool for offshore exploration, *The Leading  
307 Edge*, 25, 438-444, doi: 10.1190/1.2193225, 2006.

308 Constable, S.: Ten years of marine CSEM for hydrocarbon exploration, *Geophysics*, 75, 75A67-75A81,  
309 doi: 10.1190/1.3483451, 2010.

310 Constable, S.: Review paper: Instrumentation for marine magnetotelluric and controlled source  
311 electromagnetic sounding, *Geophysical Prospecting*, 61, 505-532, doi:  
312 10.1111/j.1365-2478.2012.01117.x, 2013.

313 Constable, S. and Srnka, L. J.: An introduction to marine controlled-source electromagnetic methods  
314 for hydrocarbon exploration, *Geophysics*, 72, WA3-WA12, doi: 10.1190/1.2432483, 2007.

315 Costa, L. G. d. S., Queiroz, A. C. M. d., Adebisi, B., Costa, V. L. R. d., and Ribeiro, M. V.: Coupling for  
316 power line communications: A survey, *Journal of Communication and Information Systems*, 32, doi:  
317 10.14209/jcis.2017.2, 2017.

318 Cox, C., Constable, S., Chave, A., and Webb, S.: Controlled-source electromagnetic sounding of the  
319 oceanic lithosphere, *Nature*, 320, 52-54, doi: 10.1038/320052a0, 1986.

320 Edwards, R. and Chave, A.: A transient electric dipole-dipole method for mapping the conductivity of  
321 the sea floor, *Geophysics*, 51, 984-987, doi: 10.1190/1.1442156, 1986.

322 Ferreira, H. C., Grové, H. M., Hooijen, O., and Vinck, A. H.: Power line communication, *Wiley  
323 Encyclopedia of Electrical and Electronics Engineering*, 16, 706-716, doi:  
324 10.1002/047134608X.W2004, 2001.

325 Giraneza, M. and Abo-Al-Ez, K.: Power line communication: A review on couplers and channel  
326 characterization, *AIMS Electronics and Electrical Engineering*, 6, 265-284, doi:  
327 10.3934/electreng.2022016, 2022.

328 Kaddoum, G. and Tadayon, N.: Differential chaos shift keying: A robust modulation scheme for  
329 power-line communications, *IEEE Transactions on Circuits and Systems II: Express Briefs*, 64, 31-35,  
330 doi: 10.1109/TCSII.2016.2546901, 2016.

331 Liu, Y., Yin, C., Weng, A., and Jia, D.: Attitude effect for marine CSEM system, *Chinese Journal of*  
332 *Geophysics*, 55, 2757-2768, doi: 10.6038/j.issn.0001-5733.2012.08.027, 2012.

333 Meng, W., Ming, D., Qi-sheng, Z., Kai, C., and Jin-ling, C. U. I.: The technique of time  
334 synchronization operation to control marine electromagnetic emission, *Progress in Geophysics*, 24,  
335 1493-1498, doi: 10.3969/j.issn.1004-2903.2009.04.043, 2009.

336 Qiu, Y., Yang, Q., Deng, M., and Chen, K.: Time synchronization and data transfer method for towed  
337 electromagnetic receiver, *Review of Scientific Instruments*, 91, doi: 10.1063/5.0012218, 2020.

338 Wang, M., Deng, M., Zhao, Q., Luo, X., and Jing, J.: Two types of marine controlled source  
339 electromagnetic transmitters, *Geophysical Prospecting*, 63, 1403-1419, doi: 10.1111/1365-2478.12329,  
340 2015a.

341 WANG, M., DENG, M., WU, Z.-L., LUO, X.-H., JING, J.-E., and CHEN, K.: New type deployed  
342 marine controlled source electromagnetic transmitter system and its experiment application, *Chinese*  
343 *Journal of Geophysics*, 60, 4253-4261, doi: 10.1111/1365-2478.12329, 2017a.

344 Wang, M., Deng, M., Wu, Z., Luo, X., Jing, J., and Chen, K.: The deep-tow marine controlled-source  
345 electromagnetic transmitter system for gas hydrate exploration, *Journal of Applied Geophysics*, 137,  
346 138-144, doi: 10.1016/j.jappgeo.2016.12.019, 2017b.

347 WANG, M., WU, Z.-L., DENG, M., MA, C.-W., LIU, Y., and WANG, S.-X.: The high precision time  
348 stamp technology in MCSEM transmission current waveform, *Progress in Geophysics*, 30, 1912-1917,  
349 doi: 10.6038/pg20150452, 2015b.

350 Wang, M., Zhang, H.-Q., Wu, Z.-L., Sheng, Y., Luo, X.-H., Jing, J.-E., and Chen, K.: Marine controlled  
351 source electromagnetic launch system for natural gas hydrate resource exploration, *Chinese Journal of*  
352 *Geophysics*, 56, 3708-3717, doi: 10.6038/cjg20131112, 2013.

353 Wang, M., Ming, D., Li, X., Zhang, Z., Yue, H., Zhang, T., Duan, N., and Ma, X.: The latest  
354 development of Marine controllable source electromagnetic transmitter, *IOP Conference Series: Earth*  
355 *and Environmental Science*, Changchun, China, 11-14 October 2020, 012137, doi:  
356 10.1088/1755-1315/660/1/012137, 2021.

357